Theoretical Study of the Copper-Catalyzed Hydroarylation of (Trifluoromethyl)alkyne with Phenylboronic Acid

Yoshihiko Yamamoto*

Department of Basic Medicinal Sciences, Graduate School of Pharmaceutical Sciences, Nagoya University, Chikusa, Nagoya 464-8601

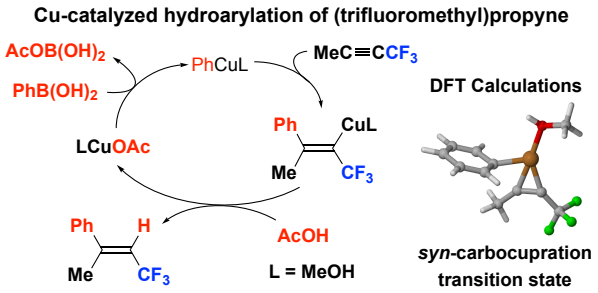

ABSTRACT

The copper-catalyzed hydroarylation of 1,1,1-trifluoro-2-butyne with phenylboronic acid was investigated by performing density functional theory calculations, and a plausible mechanism was proposed. The initial transmetalation step was first examined to compare feasibility of the catalytically active copper species. Subsequently, the carbocupration of

1,1,1-trifluoro-2-butyne by the phenylcopper species was examined in terms of regioselectivity. The impacts of the alkyne terminal group and the para substituents of phenylboronic acids on the carbocupration were also examined. Moreover, to shed light on the role of the electron-withdrawing groups on the alkyne substrates, the activation barrier for the carbocupration of 1,1,1-trifluoro-2-butyne was compared to those for several alkyne substrates bearing ester, ketone, cyano, and pentafluorophenyl groups, as well as 2-butyne, which has no electron-withdrawing group. The final protodecupration step involving methanol, acetic acid, or phenylboronic acid was examined to determine possible proton donors.

INTRODUCTION

The transition-metal-catalyzed hydroarylation of alkynes with arylboron reagents is a powerful approach to obtain arylalkenes, which are privileged structural motifs and valuable synthetic intermediates in organic chemistry.[1] Since the pioneering reports by the Hayashi group and the Shirakawa group in 2001,[2,3] various transition-metal complexes have been employed as catalysts in this reaction, and in particular, methods

using rhodium and palladium catalysts have been extensively developed. In contrast, first-row transition-metal catalysts have rarely been employed for this purpose, although they are less expensive and readily available. For example, nickel-catalyzed hydroarylations of alkynes have been independently reported by Shirakawa *et al.* and Hartwig *et al.*; however, the reaction scope has been limited to simple alkyne substrates.[3,4] The Cheng group reported the cobalt-catalyzed hydroarylation with the wider substrate scope.[5] Nevertheless, neither a synthetic application nor a detailed mechanistic study of these methods has been reported, to the best of our knowledge.

We have independently developed the copper-catalyzed hydroarylation of electron-deficient alkynes such as alkynyl esters and nitriles.[6] Our copper-catalyzed hydroarylation has several advantages: (1) aryl groups can be regioselectively introduced at the β-position relative to electron-withdrawing groups (Ewgs), (2) the aryl group and proton are stereoselectively introduced across the alkyne triple bond in a *syn* fashion, (3) diverse functional groups are tolerated, and (4) no ligands or additives are required. In addition, the copper-catalyzed hydroarylation is scalable.[7] Based on these intriguing features, copper-catalyzed hydroarylation has been combined with subsequent

cyclizations to synthesize important heterocyclic frameworks such as butenolides, pentenolides, coumarins, quinolones, and indoles.[7b,8]

Recently, we have also developed the copper-catalyzed hydroarylation of (trifluoromethyl)alkynes using arylboronic acids.[9] The reaction proceeds in a *syn* fashion at ambient temperature in MeOH, resulting in the formation of (trifluoromethyl)alkenes with aryl groups introduced at the β-position to the trifluoromethyl group. Therefore, the trifluoromethyl group behaves as the electronic directing group in a similar manner to esters and nitriles in the copper-catalyzed hydroarylation. On the basis of these experimental results, the copper-catalyzed hydroarylation has been suggested to proceed *via* (1) transmetalation between Cu(I) methoxide and an arylboronic acid, leading to an ArCu(I) species, (2) the insertion of an alkyne into the C_{Ar}–Cu bond, leading to an alkenylcopper(I) species in which the C_{vinyl}–Cu bond is stabilized by the adjacent Ewg, and (3) the final protonation of the C_{vinyl}–Cu bond by MeOH, leading to the arylalkene product as well as the restoration of Cu(I) methoxide (Scheme 1a). In association with this catalytic mechanism quite distinct from that of the relevant conjugate addition of Gilman cuprates to alkynoates,[10] the copper-catalyzed hydroarylation has practical

advantages over the conventional cuprate addition: the Cu-catalyzed hydroarylation can be conducted at room temperature in a methanol solvent to obtain products with a high *syn* selectivity, while low reaction temperature, typically –78 °C, and strictly anhydrous conditions are mandatory for conjugate addition using cuprates.

Nevertheless, the details of each fundamental step of the copper-catalyzed hydroarylation remain to be investigated. In particular, the Ewgs and the proton source are known to play highly important roles in determining the overall reaction efficiency, as well as in dictating the regio- and stereochemical outcome. In this study, to shed light on the mechanistic details, the copper-catalyzed hydroarylation of 1,1,1-trifluoro-2-butyne with phenylboronic acid was investigated by performing theoretical calculations using the density functional theory (DFT) method.

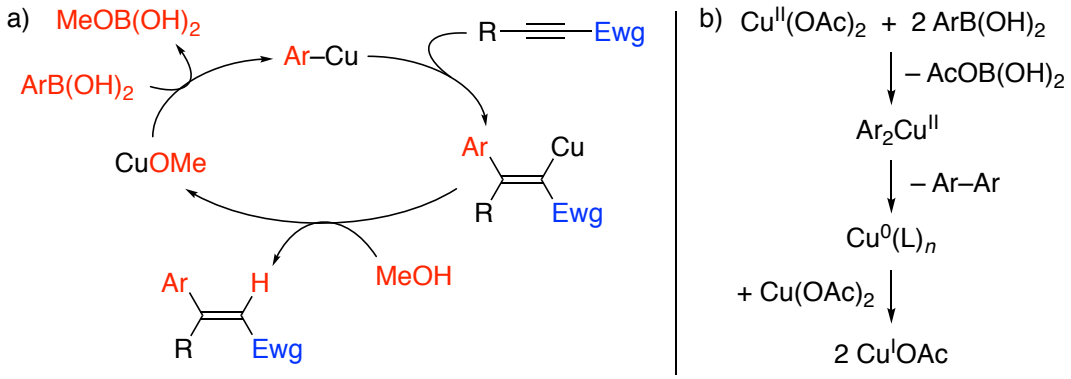

Scheme 1. Previously proposed catalytic cycle for copper-catalyzed hydroarylation.

COMPUTATIONAL METHODS

The Gaussian 16 program package was used for all calculations.[11] The geometries of the stationary points and transition states were fully optimized using Truhlar's M06L functional[12] with a double-ζ basis set with the relativistic effective core potential of Hay and Wadt (LanL2DZ)[13] for Cu and the 6-31G(d)[14] basis sets for other elements. This method was found efficient and afforded a good result of the structural optimization for a known η^2-alkyne copper complex, which was unambiguously characterized by X-ray crystallography (see, Supporting Information). The vibrational frequencies and the thermal correction to Gibbs free energy (TCGFE) including the zero-point energy were calculated at the same level of theory. The obtained structures were characterized by the number of imaginary frequencies (IF, one or zero for transition or ground states, respectively). The connectivity of each step was also confirmed by intrinsic reaction coordinate (IRC) calculations[15] from the transition states followed by optimization of the resultant geometries. Single-point energies for the geometries obtained by the above method were calculated using the Becke's three-parameter hybrid density functional method (B3LYP)[16] with a [6*s*5*p*3*d*2*f*1*g*] contracted-valence basis set with the Stuttgart-

Dresden-Bonn energy-consistent pseudopotential (SDD)[17,18] for Cu and the 6-311++G(d,p) basis sets[19] for other elements. For empirical dispersion correction, the D3 version of Grimme's dispersion with Becke-Johnson damping was also used.[20] For the solvent effects, the above single-point energy calculations were performed using the SMD model[21] with methanol as the solvent. CYLview (Ver. 1.0b)[22] was used for the visualization of the optimized structures.

RESULTS AND DISCUSSION

Boron to copper transmetalation. In our previous studies, both $Cu^{I}OAc$ and $Cu^{II}(OAc)_2$ have been used as the precatalyst; however, the hydroarylation of an alkynoate with phenylboronic acid proceeded faster when $Cu^{I}OAc$ was used than with $Cu^{II}(OAc)_2$.[6a] Therefore, the net catalyst should be a Cu(I) species, and $Cu^{II}(OAc)_2$ is presumably reduced *in situ* to a Cu(I) species by arylboron regents with their concomitant homocoupling (Scheme 1b).[23] Thus, the boron-to-copper transmetalation was first investigated using Cu(I) species. At the outset, the transmetalation starting from the precatalyst $Cu^{I}OAc$ was examined, as outlined in Scheme 2. The $Cu^{I}OAc/PhB(OH)_2$

coordination complex **1** was determined to be the precursor for the transmetalation. The acetate ligand bridges the Cu and B centers (Cu–O1 = 2.081 Å and B–O2 = 1.634 Å), with the C–O1 distance slightly shorter than that of C–O2 (1.255 Å vs. 1.283 Å). The phenyl ring coordinates to the Cu center in a η^2-fashion (Cu–C_{ipso} = 2.069 Å and Cu–C_{ortho} = 2.129 Å). In comparison to **1**, the B–C_{ipso} distance in $\mathbf{TS_{1\text{-}2}}$ was significantly elongated from 1.627 Å to 2.226 Å, and conversely, the Cu–C_{ipso} distance was shortened to 1.940 Å. The activation barrier was estimated to be $\Delta G^{\ddagger}$ = +17.5 kcal/mol, which is small enough to be overcome at ambient temperature. Finally, PhCu(MeOH) with a linear geometry and $AcOB(OH)_2$ were generated with a slight exergonicity (–0.9 kcal/mol). Thus, the transmetalation involving AcOCu(MeOH) and $PhB(OH)_2$ is kinetically feasible and thermodynamically almost neutral.

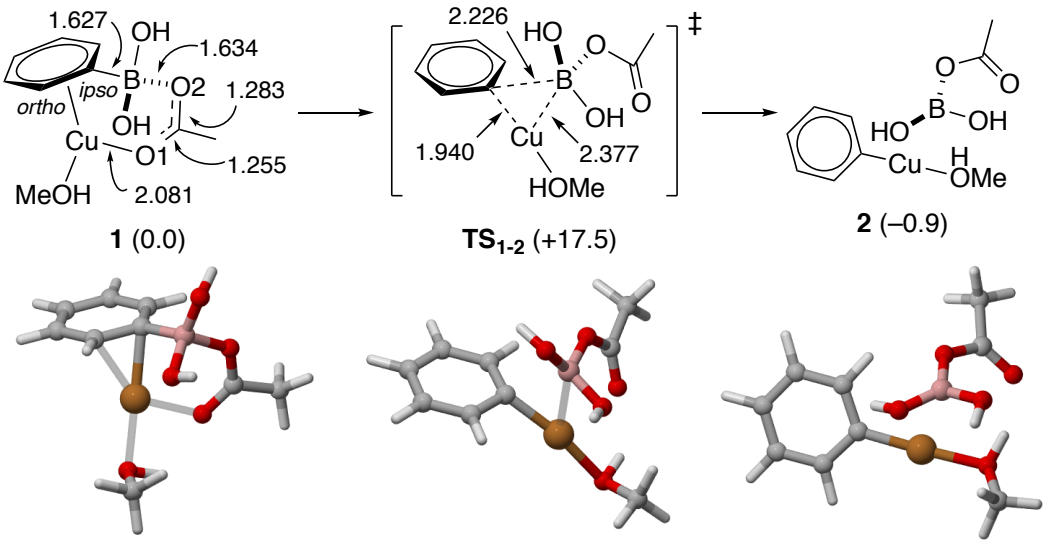

Scheme 2. Transmetalation involving AcOCu(MeOH) and $PhB(OH)_2$. Relative Gibbs free energies at 298 K are given in parentheses (kcal/mol). Interatomic distances are given in Å.

A similar transmetalation involving $Cu^{I}OMe$ rather than $Cu^{I}OAc$ was then studied, as the former has been proposed as the active catalytic species (Scheme 3). In the initial ionic complex **3**, the methoxo ligand was completely transferred from the Cu center to the B center. $\mathbf{TS_{3\text{-}4}}$ is an early transition state compared to $\mathbf{TS_{1\text{-}2}}$, as evidenced by the shorter B–C_{ipso} and longer Cu–C_{ipso} distances. The activation barrier was estimated to be $\Delta G^{‡}$ = +7.8 kcal/mol, which is much smaller than that of the above CuOAc/$PhB(OH)_2$ transmetalation. Moreover, the formation of linear PhCu(MeOH) with $MeOB(OH)_2$ was found to be exergonic by –16.1 kcal/mol. Thus, the transmetalation step involving CuOMe is kinetically and thermodynamically more feasible than that involving CuOAc.

However, the determination of the active catalyst species requires further investigations, because their feasibility in the catalytic cycle also depends on their restoration efficiency (*vide infra*).

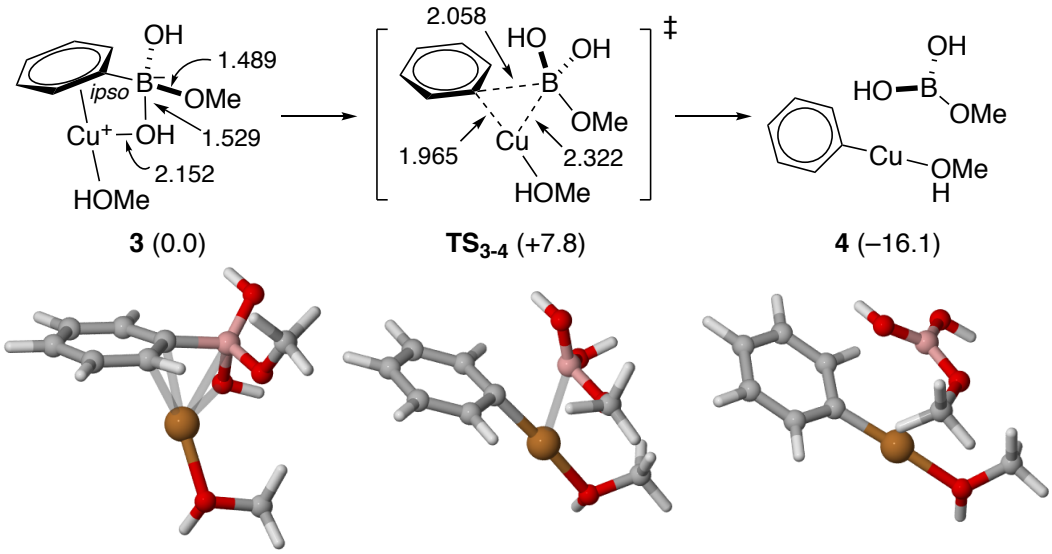

Scheme 3. Transmetalation involving MeOCu(MeOH) and $PhB(OH)_2$. Relative Gibbs free energies at 298 K are given in parentheses (kcal/mol). Interatomic distances are given in Å.

Carbocupration of alkynes. In our previous study, the aryl groups were introduced to the carbon β to the CF_3 substituent (C_β).[9] This regioselectivity is in accordance with the charge distributions of the trifluoropropyne substrate and PhCu(MeOH) species: the electronegative phenyl group is transferred to electropositive C_β (Scheme 4). In this section, the reaction of 1,1,1-trifluoro-2-butyne with PhCu(MeOH) was examined to

discuss the regioselectivity in detail. The carbocupration with the experimentally observed regioselectivity starts from the η^2-alkyne complex **5a**, in which the alkyne, the phenyl *ipso* carbon atom (C_{ipso}), and the methanol oxygen atom are located in the same plane. The difference between the Cu–C_α and Cu–C_β distances is small (1.956 vs. 1.950 Å), and the C_α–C_β bond length is elongated from 1.208 Å in the free alkyne to 1.263 Å in **5a**, owing to back donation from the Cu center to the triple bond. In comparison to **5a**, the C_β–C_{ipso} distance significantly decreased from 3.349 Å to 2.103 Å in $\mathbf{TS_{5a\text{-}6a}}$, while the Cu–$C_{ipso}$ distance increased from 1.954 Å to 2.006 Å. In addition, the Cu–C_α distance was shortened to 1.934 Å, while the Cu–C_β distance was elongated to 1.994 Å. A reasonable activation barrier of $\Delta G^{\ddagger}$ = +19.1 kcal/mol was estimated for this step. The final formation of the carbocupration product **6a** is significantly exergonic (–39.8 kcal/mol). The Cu–C_α bond length is 1.890 Å, and the introduced phenyl group and the Cu center are mutually *cis*. Subsequently, carbocupration with the inverse regioselectivity was also investigated, and the similar starting η^2-alkyne complex **7** was located at 1.9 kcal/mol above **5a**. Furthermore, the Cu–C_α distance in **7** is shorter than the Cu–C_β distance in **5** (1.918 vs. 1.950 Å), while the Cu–C_β distance in **7** is significantly longer

(2.029 Å), owing to the reduced back donation from the Cu center to C_β in the absence of an Ewg. In $\mathbf{TS_{7\text{-}8}}$, the Cu–C_α and Cu–C_β distances are 1.948 and 1.953 Å, respectively. Accordingly, the transformation of **7** into $\mathbf{TS_{7\text{-}8}}$ requires significant distortion, in particular, a substantial shortening of the Cu–C_β distance by 0.075 Å, resulting in a larger activation barrier of $\Delta G^{\ddagger}$ = +27.0 kcal/mol. The formation of **8** from **7** is less exergonic (–31.9 kcal/mol) than that of **6a** from **5a**. The difference in exergonicity is ascribable to the different stabilities of the products: **6a** is more stable than **8** because of the stronger Cu–C_{vinyl} bond, as evidenced by the Cu–C_α distance in **6a** (1.890 Å) and the Cu–C_β distance in **8** (1.901 Å). Overall, the carbocupration with the inverse regioselectivity is both kinetically and thermodynamically less favorable.

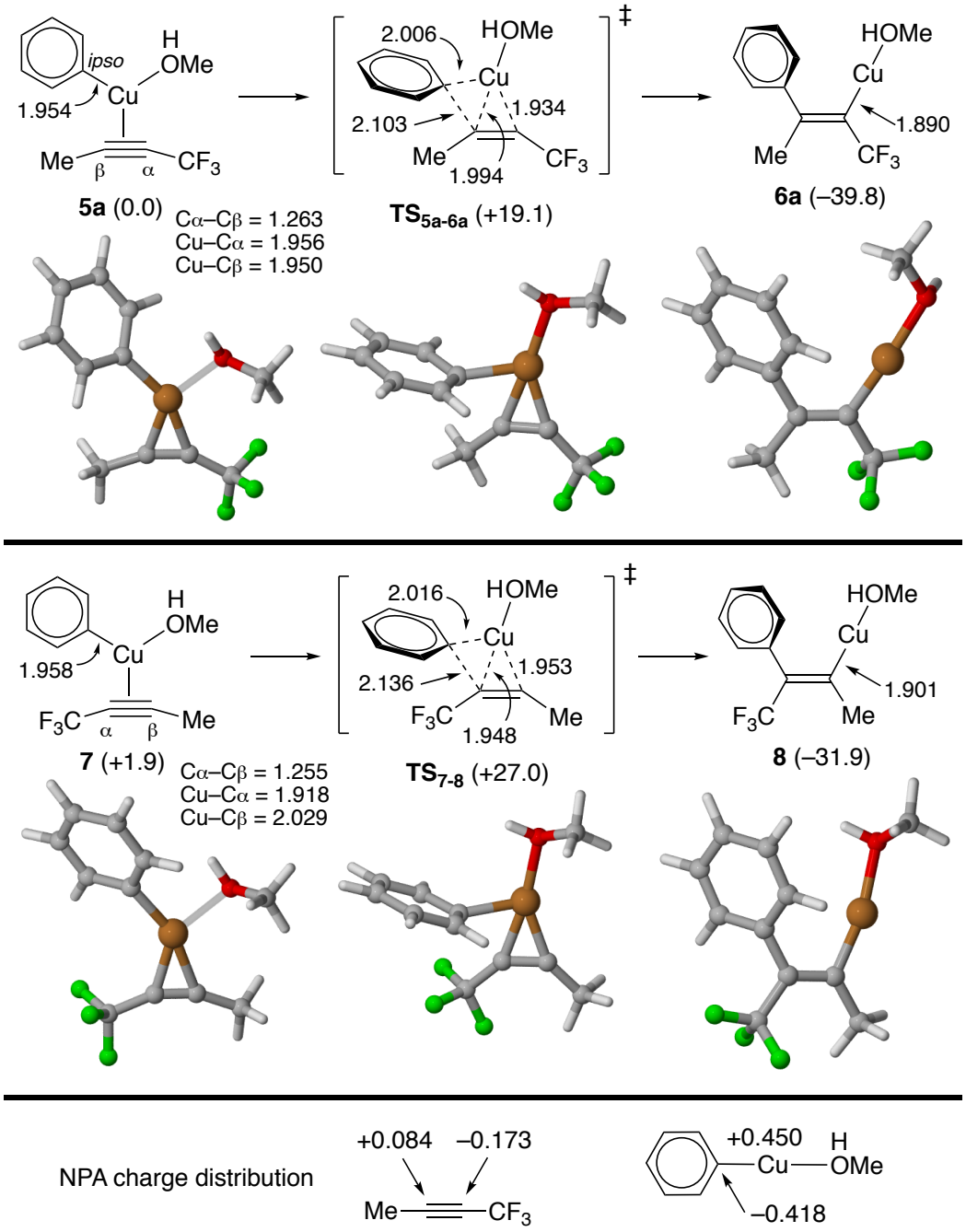

Scheme 4. Carbocupration of 1,1,1-trifluoro-2-butyne with PhCu(MeOH). Relative Gibbs free energies at 298 K are given in parentheses (kcal/mol). Interatomic distances are given in Å.

The electronic influence of the *para* substituent of the phenylboronic acids on the

carbocupration efficiency was briefly investigated by computing the reactions with copper complexes bearing the *p*-anisyl and *p*-nitrophenyl ligands as representative electron-rich and electron-deficient aryl groups, respectively. In our previous experimental work, electron-deficient arylboronic acids were found to be inferior to electron-neutral and -rich ones. In good accordance with this empirical reactivity trend, the calculated activation barrier is 3.3 kcal/mol higher for the *p*-nitrophenyl derivative than the electron-neutral phenyl derivative, while that of the electron-rich *p*-anisyl derivative is slightly lower than that of the phenyl derivative (Table 1, entries 2 and 3). In addition, the reaction exergonicity (ΔG_{rxn}) decreased in the order *p*-anisyl > Ph > *p*-nitrophenyl.

Table 1. Reaction parameters for the carbocupration of electron-deficient alkynes.

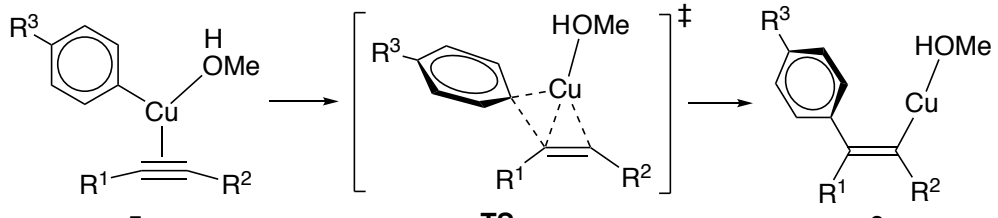

5 **$TS_{5\text{-}6}$** **6**

Entry	Model LUMO (eV)[a]	σ_p[b]	$\Delta G^{‡}/\Delta G_{rxn}$ (kcal/mol)
1	R^1 = Me, R^2 = CF_3, R^3 = H (**a**) –0.00964	0.54	+19.1/–39.8
2[c]	R^1 = Me, R^2 = CF_3, R^3 = OMe (**a**/**OMe**)	0.54	+18.4/–41.2

	–0.00964		
3[c]	R^1 = Me, R^2 = CF_3, R^3 = NO_2 (**a**/**NO_2**) –0.00964	0.54	+22.4/–37.0
4	R^1 = Ph, R^2 = CF_3, R^3 = H (**b**) –0.07255	0.54	+19.7/–40.5
5	R^1 = Me, R^2 = C_6F_5, R^3 = H (**c**) –0.06487	0.27	+21.7/–35.2
6	R^1 = Me, R^2 = CO_2Me, R^3 = H (**d**) –0.05534	0.45	+18.7/–36.8
7	R^1 = Me, R^2 = COMe, R^3 = H (**e**) –0.07074	0.50	+17.9/–30.7
8	R^1 = Me, R^2 = CN, R^3 = H (**f**) –0.06329	0.66	+17.4/–42.9
9	R^1 = R^2 = Me, R^3 = H (**g**) –0.04497	–0.17	+38.7/–19.9

[a] LUMO for free alkynes. [b] Hammett substituent constants for R^2 reported in ref. 26.
[c] Reactions of *p*-anisyl (entry 2) and *p*-nitrophenyl (entry 3) derivatives were calculated.

In the experimental study of the Cu-catalyzed hydroarylation of (trifluoromethyl)alkynes, mainly aryl groups were employed as the alkyne terminal groups,[9] because of their ease of preparation by the trifluoromethylation of the corresponding arylalkynes.[24] Thus, the impact of the terminal phenyl substituent on the carbocupration efficiency was also examined, as shown in Scheme 5. The results obtained were very similar to those of the carbocupration of (trifluoromethyl)propyne discussed above (Table 1, entries 1 and 4). In the initial η^2-alkyne complex **5b**, the terminal phenyl ring and the Cu–alkyne moiety are

in the same plane to maximize the π-conjugation. However, from **5a** to $\mathbf{TS_{5b\text{-}6b}}$, the terminal phenyl group rotated to mitigate the steric repulsion from the transferred phenyl ligand. Nevertheless, the C_{ipso}–Cβ distance in $\mathbf{TS_{5b\text{-}6b}}$ (2.136 Å) is longer than that in $\mathbf{TS_{5a\text{-}6a}}$ (2.103 Å), while other steric parameters are similar. The activation barrier for the carbocupration of **5b** and the exergonicities for the formation of **6b** are almost the same with the corresponding values for the reaction of **5a**.

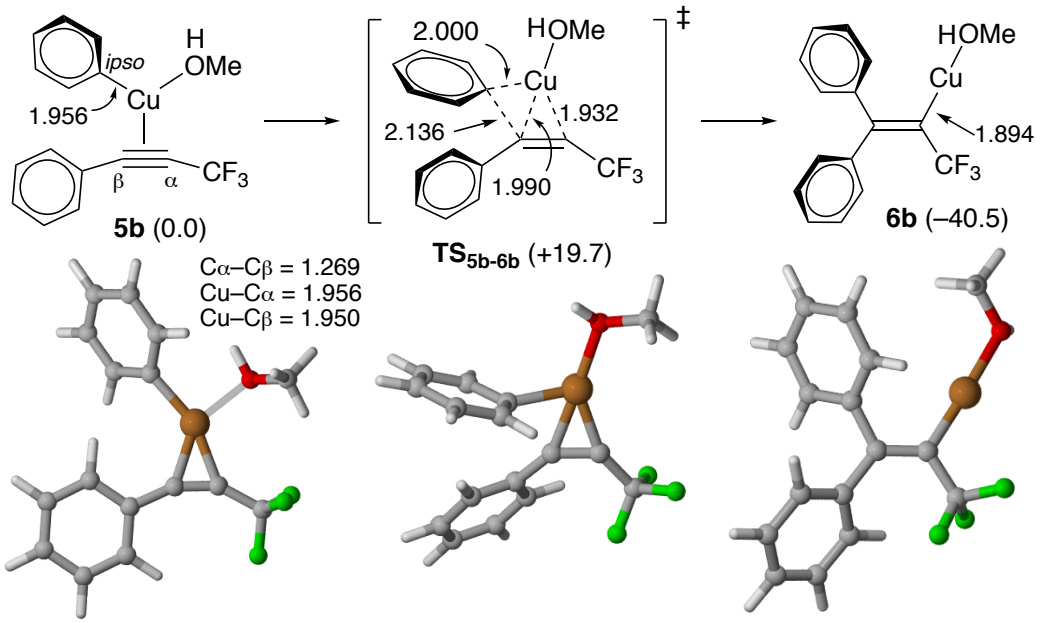

Scheme 5. Carbocupration of (trifluoromethyl)alkyne bearing a terminal phenyl group with PhCu(MeOH). Relative Gibbs free energies at 298 K are given in parentheses (kcal/mol). Interatomic distances are given in Å.

Next, the influence of the Ewgs on the efficiency of the carbocupration step was examined.

The carbocuprations of propyne derivatives bearing a pentafluorophenyl, methoxycarbonyl, acetyl, or cyano group as the Ewgs were analyzed. The obtained activation barriers ($\Delta G^{‡}$) and exergonicities (ΔG_{rxn}) are summarized in Table 1 (entries 5–8). Previously, the hydroarylation of 1,2,3,4,5-pentafluoro-6-(3-methoxy-1-propynyl)benzene with (*p*-chlorophenyl)boronic acid (2 equiv) was performed using 10 mol% $Cu(OAc)_2$ in MeOH at 28 °C for 3 h, resulting in the 60% recovery of the alkyne along with the desired product (in less than 20% yield).[25] This result showed that the pentafluorophenyl substituent is an inferior Ewg compared to the trifluoromethyl substituent. In accordance with this observation, DFT calculations of the carbocupration of the (pentafluorophenyl)propyne estimated an activation barrier of $\Delta G^{‡}$ = +21.7 kcal/mol, which is 2.6 kcal/mol higher than that of the trifluoromethyl analog (entry 5). Similarly to (trifluoromethyl)alkynes, alkynyl esters and nitriles have also proven to be efficient substrates in our previous studies.[6] Calculations of the model reactions for the methoxycarbonyl- and cyano-substituted propynes afforded activation barriers lower than that of the (trifluoromethyl)propyne (entries 6 and 8). In particular, the smallest activation barrier ($\Delta G^{‡}$ = +17.4 kcal/mol) was obtained for the carbocupration of 1-cyanopropyne

(entry 8). The data summarized in Table 1 suggest that the trend in the carbocupration efficiency correlates with the Hammett substituent constant (σ_p)[26] of the Ewgs rather than the LUMO level of the free alkyne substrates. The importance of the Ewgs in Cu-catalyzed hydroarylation was well demonstrated by calculations of the carbocupration of 2-butyne (Scheme 6 and Table 1, entry 9). The electron-deficient alkynes form tri-coordinated copper complexes **5a**–**f**, in which the phenyl ligand and C_β are located in close proximity. In contrast, 2-butyne affords the di-coordinated complex **5g** with a non-coordinated MeOH molecule. The alkyne moiety is almost linear, as indicated by the C_{Me}–C_β–C_α–C_{Me} dihedral angle of 2.6°. The C_{ipso}–C_β distance is considerably long at 3.931 Å. Thus, a drastic structural change is required to transform **5g** into $\mathbf{TS_{5g\text{-}6g}}$, resulting in a very high activation barrier of $\Delta G^{\ddagger}$ = +38.7 kcal/mol. The formation of **6g** from **5g** is much less exergonic (–19.9 kcal/mol) than that of **6a** from **5a** (–39.8 kcal/mol).

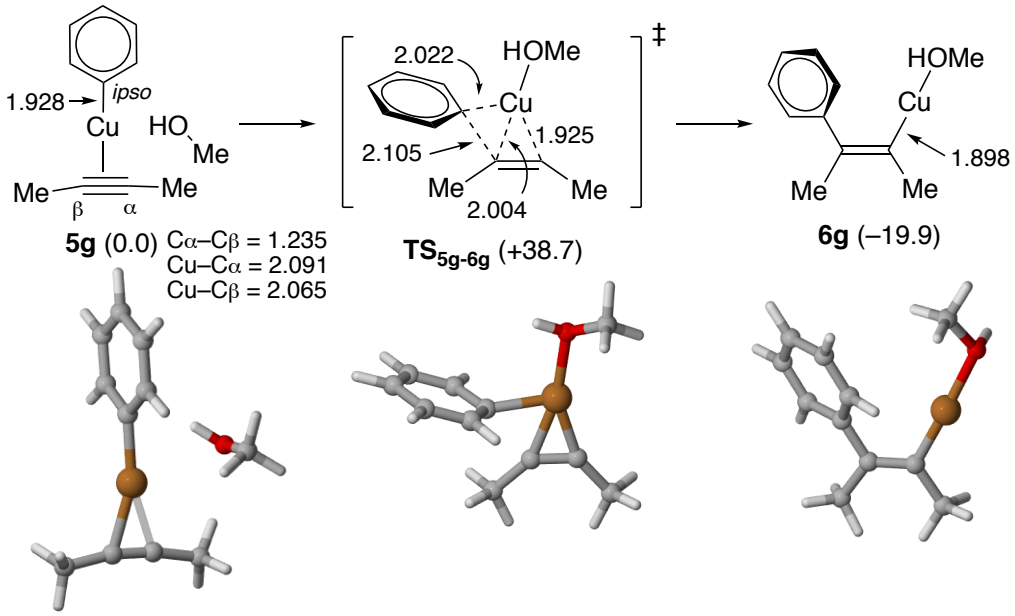

Scheme 6. Carbocupration of 2-butyne with PhCu(MeOH). Relative Gibbs free energies at 298 K are given in parentheses (kcal/mol). Interatomic distances are given in Å.

Protodecupration of the vinylcopper intermediate. The protonation of the vinylcopper intermediate leads to the formation of the final hydroarylation product with the concomitant restoration of the catalytically active copper species. The methanol solvent has been considered to be the net proton source, as confirmed by control experiments in which the use of MeOD as the solvent produced the deuterated product.[6a] Thus, at the outset, an external methanol molecule was used as the proton donor for the vinylcopper intermediate derived from (trifluoromethyl)propyne (Scheme 7). As expected, **TS9-10** could be located for the protodecupration starting from the initial state **9**, and after passing through the transition state, the η^2-copper complex **10** of the resultant hydroarylation

product (Cu–C_α = 1.984 Å and Cu–C_β = 2.053 Å) was generated. From **9** to **$TS_{9\text{-}10}$**, the Cu–C_α bond was elongated from 1.892 Å to 2.008 Å, and the Cu center moved significantly outside the alkene plane, as evidenced by the C_{ipso}–C_β–C_α–Cu dihedral angle of 39°. The C_α–H and Cu–H distances of 1.310 and 1.962 Å, respectively, indicate that the proton interacts with the Cu–C_α σ-bond. Although this protonation pathway involving a methanol molecule was seemingly reasonable, the activation barrier of $\Delta G^{\ddagger}$ = +24.8 kcal/mol was relatively large. Thus, alternative proton sources were sought.

Acetic acid derived from the CuOAc precatalyst was proposed as a possible proton source because its acidity is higher than that of methanol (p*K*a: MeOH ca. 15; AcOH ca. 5). Actually, a similar transition state, **$TS_{11\text{-}12}$**, was found, and the smaller activation barrier was estimated to be $\Delta G^{\ddagger}$ = +8.0 kcal/mol (Scheme 7). In **$TS_{11\text{-}12}$**, the Cu–C_α (1.980 Å) and C_α–H (1.450 Å) distances are shorter and longer, respectively, than the corresponding distances in **$TS_{9\text{-}10}$**. This fact indicates that **$TS_{11\text{-}12}$** is an early TS compared to **$TS_{9\text{-}10}$**. Moreover, the interaction of the carbonyl oxygen of acetic acid with the Cu center (Cu–O = 2.193 Å) probably contributes to the stabilization of **$TS_{11\text{-}12}$**. The formation of η^2-alkene complex **12** proved to be more exergonic than that of **10**. In **12**, the acetate ligand

adapts a distorted κ^2 coordination (Cu–O1 = 2.034 Å, Cu–O2 = 2.368 Å, $C_{carbonyl}$–O1 = 1.286 Å, and $C_{carbonyl}$–O2 = 1.254 Å). Electron donation from the κ^2-acetato ligand to the Cu center leads to the longer Cu–C_α and Cu–C_β distances (2.009 and 2.074 Å, respectively) compared to those in **10**. Consequently, protonation involving acetic acid was estimated to be both kinetically and thermodynamically more favored than that involving methanol as the proton source.

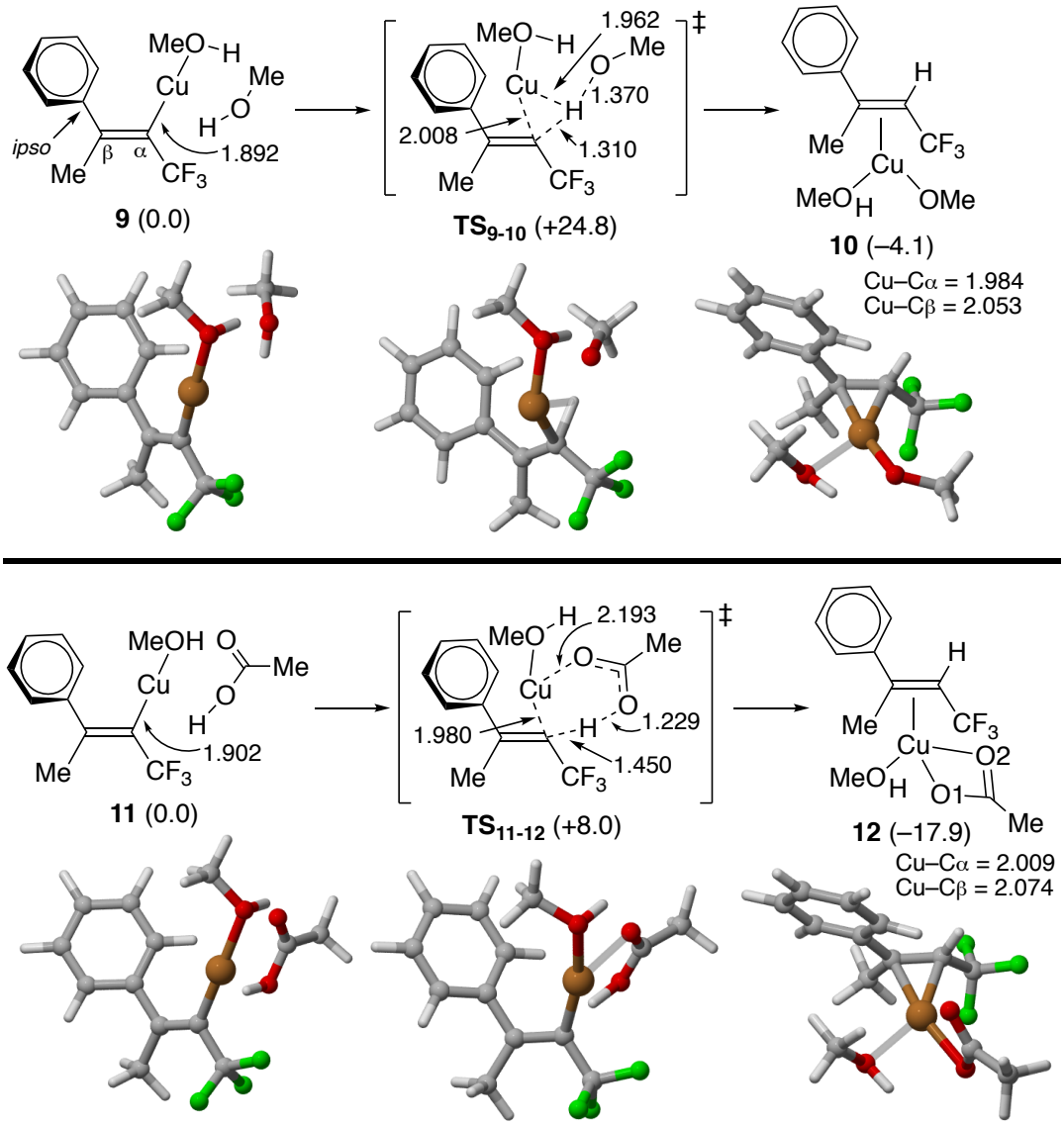

Scheme 7. Protonation of the vinylcopper intermediate with methanol or acetic acid. Relative Gibbs free energies at 298 K are given in parentheses (kcal/mol). Interatomic distances are given in Å.

According to the above results, acetic acid behaves as a superior proton donor compared to methanol. However, the role of acetic acid in protodecupration should be limited by its low concentration; only a catalytic amount of acetic acid exists under the experimental

conditions. Thus, the protonation with phenylboronic acid was also examined, as an excess of the arylboronic acids is usually used, and the acidities of arylboronic acids (p*K*a ca. 9) are close to that of phenol.[27] In fact, we observed the considerable decrease of the reaction rate when a phenylboronate was used instead of the parent phenylboronic acid.[6a] A reasonable activation barrier of $\Delta G^{\ddagger}$ = +18.3 kcal/mol was estimated for the protonation of the vinylcopper intermediate with phenylboronic acid (Scheme 8). It should be noted that the vinylcopper moiety in **TS$_{13\text{-}14}$** is significantly distorted, as indicated by the small Cu–C$_\alpha$–C$_\beta$ angle of 82.2° and short Cu–C$_\beta$ distance of 2.272 Å. The extra hydroxy group of the boronic acid is in close proximity to the Cu center, with a Cu–O distance of 2.317 Å. The Cu–C$_\alpha$ and C$_\alpha$–H distances are 1.997 and 1.465 Å, respectively, which are slightly longer than the corresponding distances in **TS$_{11\text{-}12}$**. The formation of η^2-alkene complex **14** (Cu–C$_\alpha$ = 2.015 Å, Cu–C$_\beta$ = 2.069 Å) is exergonic by 12.6 kcal/mol. These results suggest that phenylboronic acid can function as the proton donor, albeit with moderate efficiency. Therefore, it can be assumed that acidic molecules such as acetic acid, phenylboronic acid, and even other boric acid[28] residues enable protodecupration in copper-catalyzed hydroarylations.

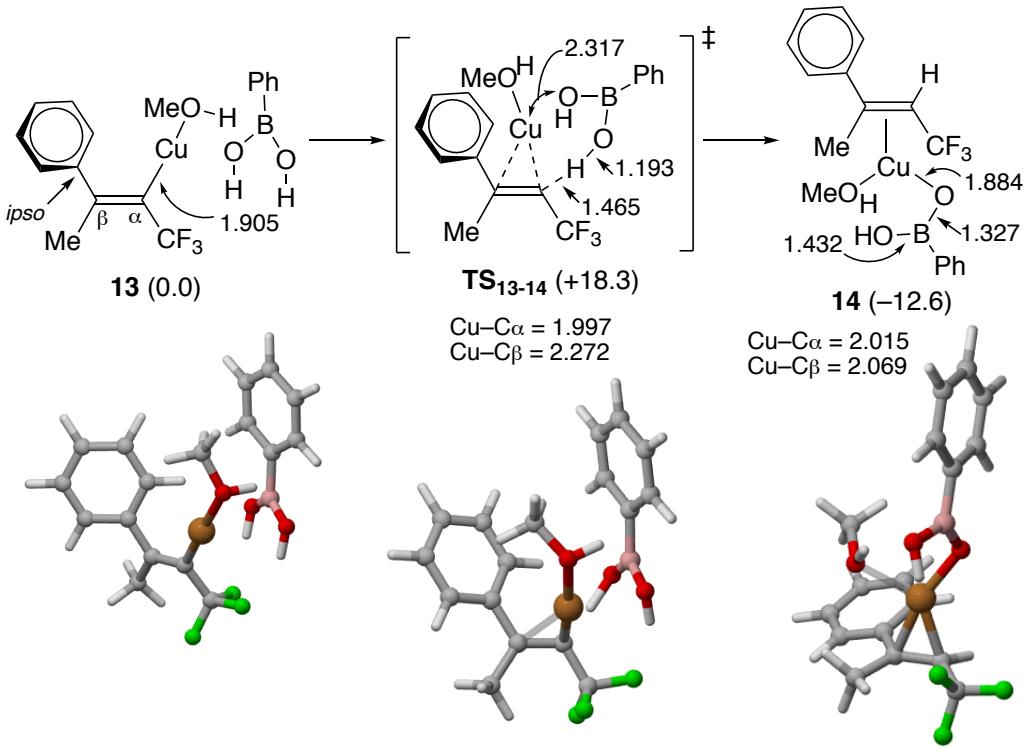

Scheme 8. Protonation of the vinylcopper intermediate with phenylboronic acid. Relative Gibbs free energies at 298 K are given in parentheses (kcal/mol). Interatomic distances are given in Å.

Stereoselectivity for hydroarylation of alkynyl ketones. The carbocupration of alkynyl ketones deserves further discussion. In our previous study, the reaction of 1-hexynyl phenyl ketone with phenylboronic acid afforded a mixture of the corresponding *syn*- and *anti*-hydroarylation products in a high combined yield with a *syn*/*anti* ratio of 86:14 (Scheme 9).[6a] This erosion of the stereoselectivity was ascribed to the *E*/*Z* isomerization of the vinylcopper intermediate *via* allenolate **15** based on precedents in the literature.[29]

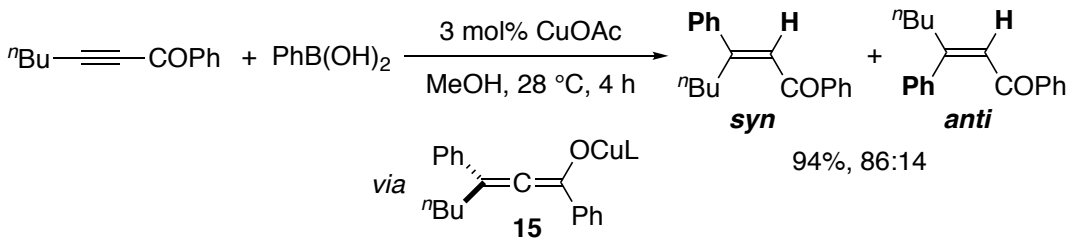

Scheme 9. Copper-catalyzed hydroarylation of benzoylalkyne with phenylboronic acid.

Thus, the carbocupration of the model substrate 1-propynyl methyl ketone was examined in detail (Table 1, entry 7 and Scheme 10). First, the normal carbocupration pathway starting from the η^2-alkyne complex **5e** was found to be kinetically feasible with a reasonable activation barrier of $\Delta G^{\ddagger}$ = +17.9 kcal/mol. The formation of vinylcopper intermediate **6e** is also thermodynamically favored, with an exergonicity of –30.7 kcal/mol. Nevertheless, further analysis led to an alternative pathway with a lower activation barrier; the PhCu(MeOH) species undergoes direct conjugate addition to the alkynyl ketone with concomitant transfer of the proton from the ligated methanol to the carbonyl oxygen atom *via* $\mathbf{TS_{16\text{-}17}}$, resulting in the formation of η^2-allenol complex **17**. In $\mathbf{TS_{16\text{-}17}}$, the Cu–$C_\beta$ distance is significantly shorter than the Cu–C_α distance (2.096 and 2.558 Å, respectively). The C_{ipso}–C_β distance is 2.117 Å, which is similar to that of $\mathbf{TS_{5e\text{-}6e}}$ (2.113 Å). The C_{Me}–C_β–C_α–$C_{carbonyl}$ dihedral angle is 171.8°. In allenol complex **17**, the Cu–C_α and Cu–C_β distances are 1.939 and 2.135 Å, respectively, indicating the η^2-

coordination mode. Due to the backdonation from the Cu center, the C_α–C_β bond was longer than the C_α–$C_{carbonyl}$ bond (1.373 and 1.338 Å, respectively). The allene moiety is almost linear (C_β–C_α–$C_{carbonyl}$ = 161.6°). The facile proton transfer from the allenol hydroxy group to the methoxo ligand on the Cu center enables the isomerization of **17** to the *anti*-carbocuparation intermediate **18** *via* $\mathbf{TS_{17\text{-}18}}$. The rotation of the methoxide ligand in **17** afforded allenol complex **19**, which underwent proton transfer *via* $\mathbf{TS_{19\text{-}20}}$ to generate *syn*-carbocupration intermediate **20**. Because the activation barriers of these proton transfers are quite small and vinylcopper species **18** and **20** are only slightly more stable than allenol complexes **17** and **19**, **18** and **20** are in rapid equilibrium.

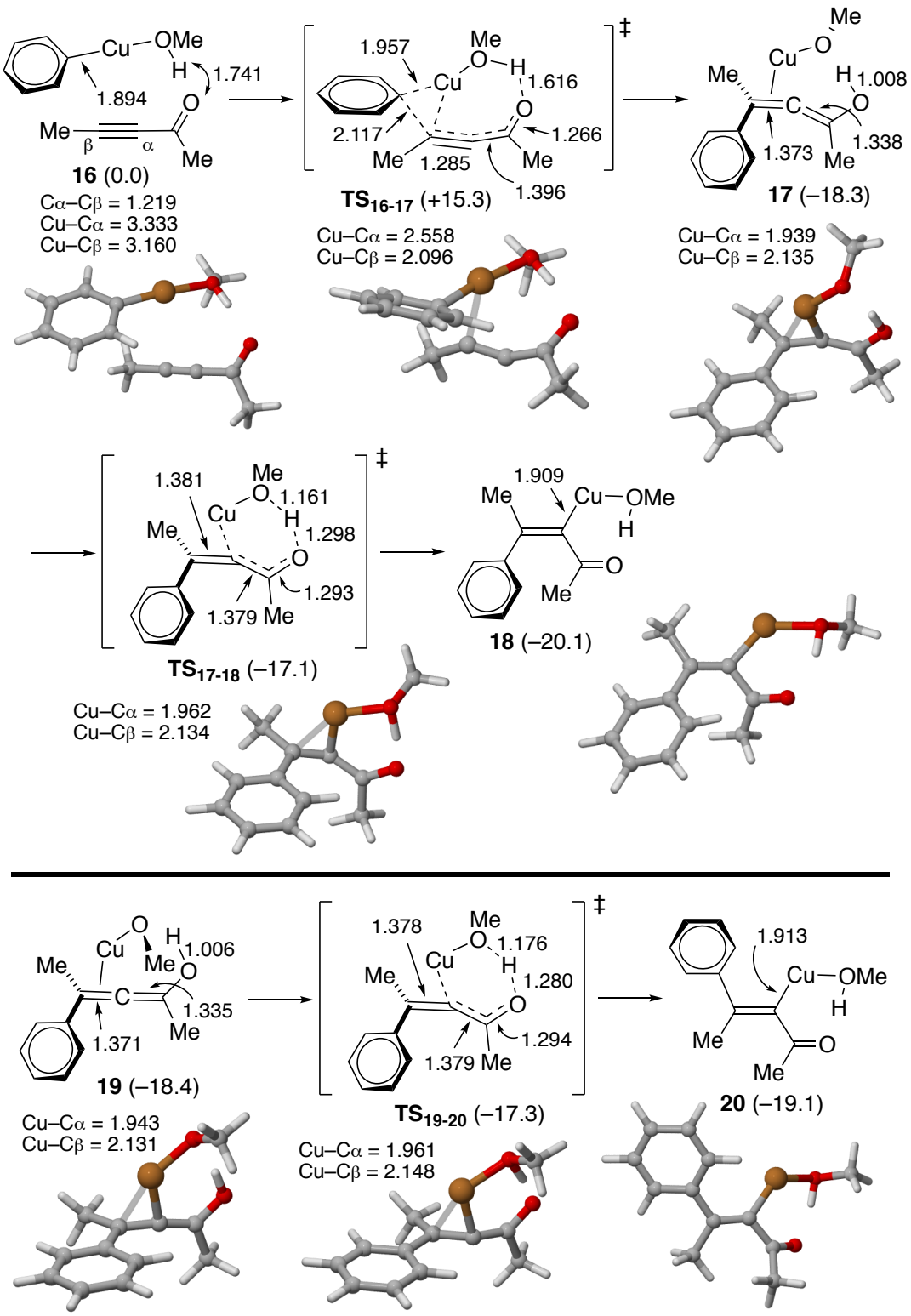

Scheme 10. Conjugate arylation of 1-propynyl methyl ketone with PhCu(MeOH) and subsequent isomerization of allenol complexes. Relative Gibbs free energies at 298 K are given in parentheses (kcal/mol). Interatomic distances are given in Å.

Further protodecupration of the vinylcopper intermediates with acetic acid was investigated, as shown in Scheme 11.[30] Protodecupration of *syn*- and *anti*-carbocupration intermediates **21** and **23** bearing a ligated acetic acid proceeded *via* $\mathbf{TS_{21\text{-}22}}$ and $\mathbf{TS_{23\text{-}24}}$, respectively, with small activation barriers. The formations of the final hydroarylation products **22** and **24** with the concomitant generation of AcOCu(MeOH) were highly exergonic (ca. –21 kcal/mol). Accordingly, the protodecupration step is both kinetically and thermodynamically feasible, and the conversion of the *syn*-carbocupration intermediate is more efficient than that of the *anti*-counterpart. Because protodecupration is the irreversible and stereo-determining step, the *syn*/*anti* ratio can be roughly estimated as *syn*/*anti* = 3:1 based on the difference in the energetic spans between the TSs and most stable vinylcopper intermediate **21**.[31] Therefore, these calculation data qualitatively support the formations of hydroarylation stereoisomers in favor of *syn*-products from alkynyl ketone substrates.

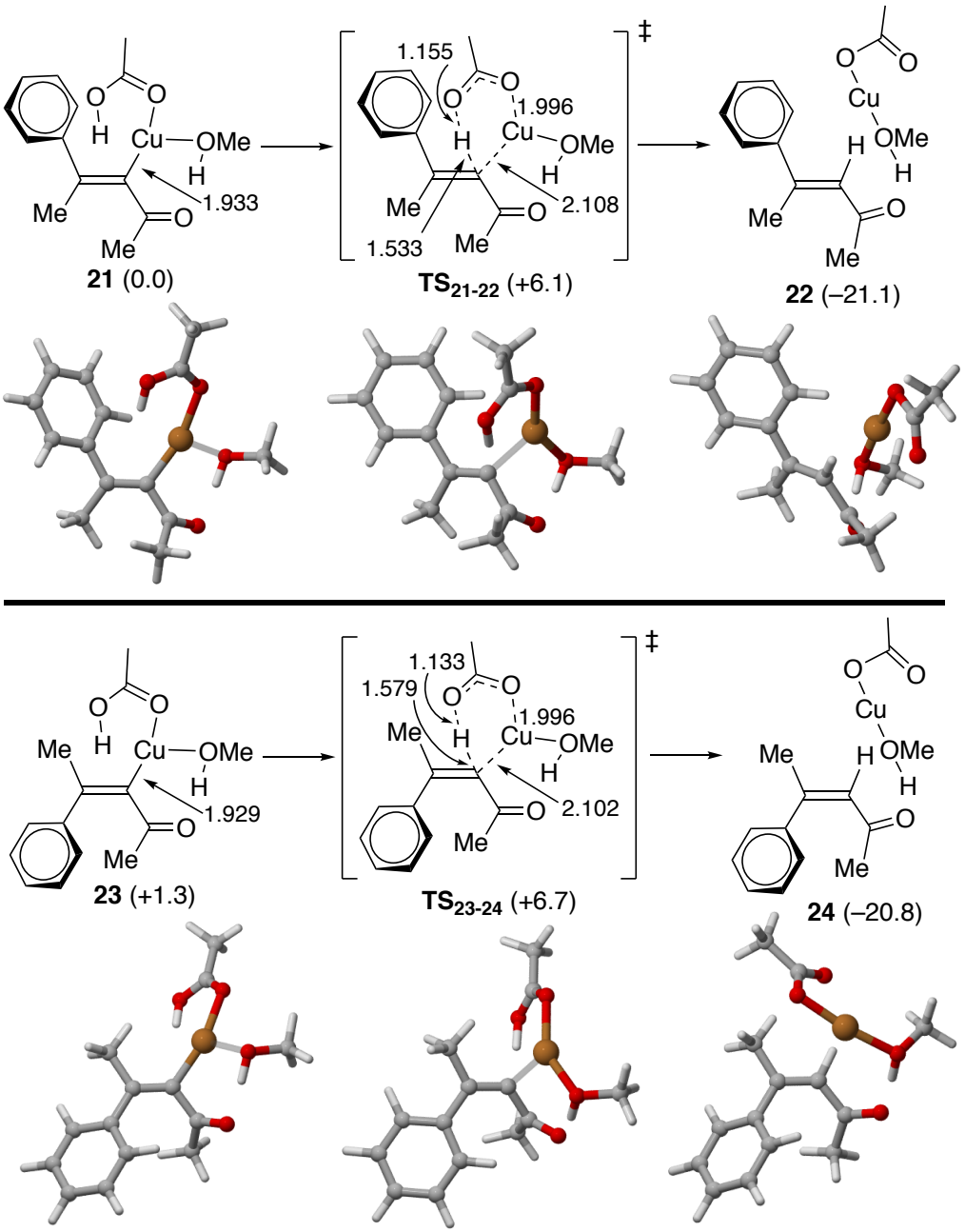

Scheme 11. Protonation of the vinylcopper intermediates derived from conjugate allylation with acetic acid. Relative Gibbs free energies at 298 K are given in parentheses (kcal/mol). Interatomic distances are given in Å.

Transmetalation and carbocupration involving Cu(II) complexes. Although the reaction mechanism involving Cu(I) species is reasonable, the feasibility of an alternative

Cu(II) pathway was also inspected. For computational efficiency, one of the acetate ligands was displaced with a formate ligand. First, transmetalation involving a Cu^{II} species was compared to that involving $Cu^{I}OAc$ (Scheme S1, Supporting Information). The initial complex **S5** has a similar acetate-bridged structure with the corresponding complex **1** except for the absence of the interaction between the Cu center and the phenyl ligand in **S5**. The activation barrier was estimated to be $\Delta G^{\ddagger}$ = +21.5 kcal/mol, which is 4 kcal/mol higher than that of the CuOAc/$PhB(OH)_2$ transmetalation. The marked difference is the higher endergonicity (+10.2 kcal/mol) of the formation of $PhCu^{II}(\kappa^2$-OCHO) with $AcOB(OH)_2$. Thus, the transmetalation involving Cu(II) species is thermodynamically infeasible. The subsequent reaction of $PhCu^{II}(\kappa^2$-OCHO) with (trifluoromethyl)propyne was found completely different with that of $PhCu^{I}$(MeOH) (Scheme S2, Supporting Information). In the initial state **S7**, the Cu center has no interaction with the alkyne triple bond, and the phenyl group was directly transferred to C_β *via* $\mathbf{TS_{S7\text{-}S8}}$ with an activation barrier of $\Delta G^{\ddagger}$ = +19.3 kcal/mol. In $\mathbf{TS_{S7\text{-}S8}}$, the alkyne moiety distorted in such a way that the terminal trifluoromethyl group moved in the opposite way to the methyl group. As a result, *anti*-carbocupration product **S8** was formed

with high exergonicity. This *trans* addition can be ascribed to the radical mechanism, in which the phenyl radical moved from the Cu(II) center to C_β and the developed C_α radical center underwent the recombination with the resultant Cu(I) fragment. The radical character $\mathbf{TS_{S7\text{-}S8}}$ was suggested by its SOMO orbital and spin density representations (Figure S2, Supporting Information). Although the activation barrier of the *anti*-carbocupration is reasonably low, the Cu(II) pathway is infeasible because the energy span between **S5** and $\mathbf{TS_{S7\text{-}S8}}$ is as high as +32.0 kcal/mol (Figure S3, Supporting Information).[31] Therefore, this Cu(II) mechanism can be excluded.

CONCLUSIONS

Copper-catalyzed hydroarylation was investigated by performing the DFT calculations of model substrates. A reaction profile for the hydroarylation of (trifluoro)propyne with phenylboronic acid was formulated, and is shown in Figure 1. In the catalytic cycle involving CuOAc as the catalytic active species, the carbocupration step is considered to be rate determining, and the largest energetic penalty of +19.1 kcal/mol is expected for this step. The barrier height can vary depending on the electronic property of the aryl

group transferred. Electron-rich aryl groups are more facilely transferred than electron-deficient counterparts. The second crucial step is the initial transmetalation. The transmetalation generates mixed anhydride $AcOB(OH)_2$, which presumably reacts with methanol to produce boric acid monoester $MeOB(OH)_2$ and acetic acid.[32] The acetic acid thus produced was expected to be the most promising proton donor in the protodecupration step, although its concentration is much lower than methanol. As an alternative option, phenylboronic acid was also suggested to be a moderately efficient proton donor. Because the activation barriers associated with each step are small enough to be overcome under the experimental conditions, and the formation of the final alkene complex **12** from the initial arene complex **1** is highly exergonic (–57.2 kcal/mol), the overall transformation is both kinetically and thermodynamically feasible.

In contrast, an alternative catalytic cycle involving CuOMe as the active catalytic species is less likely because of the inefficient protodecupration step involving MeOH: the energetic span between **6a** and $\mathbf{TS_{9\text{-}10}}$ (+30.5 kcal/mol) is too large to overcome under the experimental conditions (Figure S4 Supporting Information).[31] A more efficient pathway can be realized by combining transmetalation involving CuOMe and protodecupration

involving AcOH as shown in Figure S5 (Supporting Information) when CuOMe can be restored from CuOAc species generated in the protodecupration step. However, such a ligand exchange step could not be identified in this study.

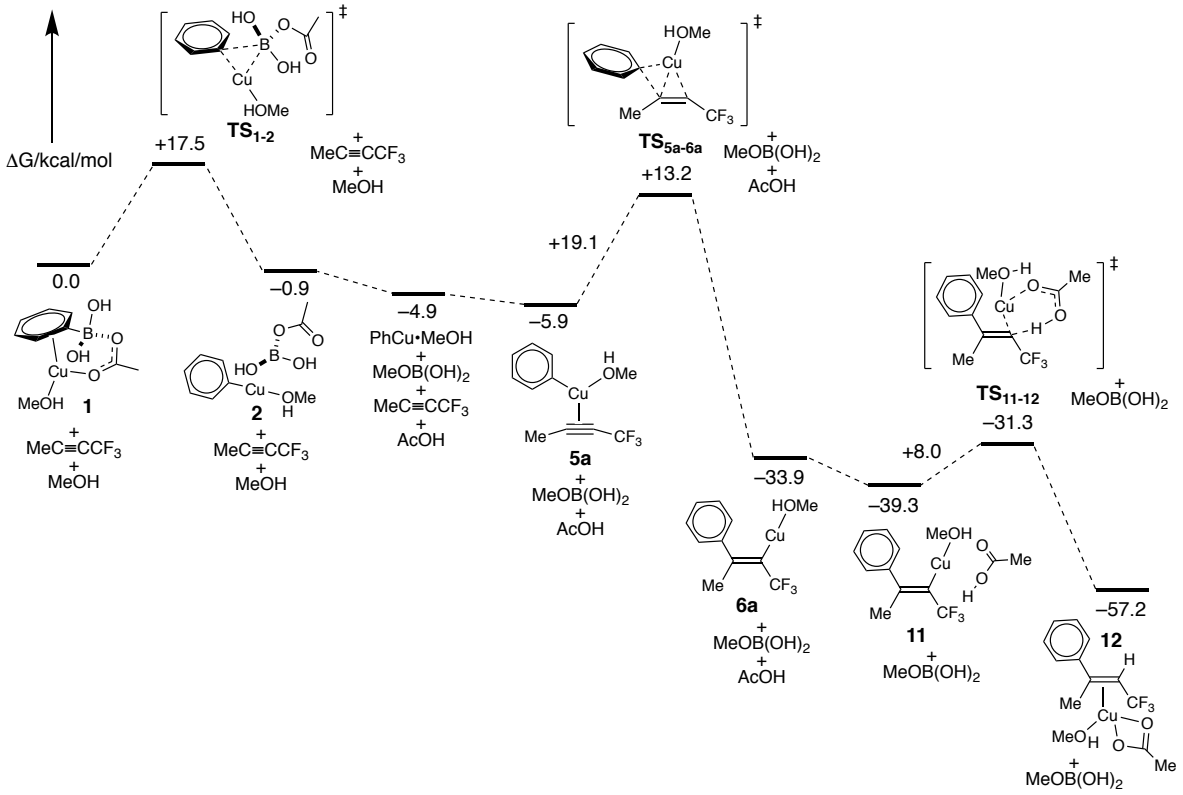

Figure 1. Energy profiles for the hydroarylation of (trifluoromethyl)propyne and phenylboronic acid involving CuOAc with relative Gibbs free energies at 298 K.

On the basis of these results, a modified catalytic cycle was proposed and is shown in Scheme 12. Moreover, a comparison of the carbocuprations of several electron-deficient alkynes suggests that the trifluoromethyl group is as efficient as the methoxycarbonyl,

acetyl, and cyano groups, and that the cyano group is the most efficient. In contrast, the pentafluorophenyl group is much less effective as the Ewg. Analysis of the acetylated propyne led to two distinct mechanisms; one is the normal carbocupration and the other is the conjugate-addition-type reaction. The latter was found only for the alkynyl ketone substrate, and is considered to be the cause of the *anti*-hydroarylation product.

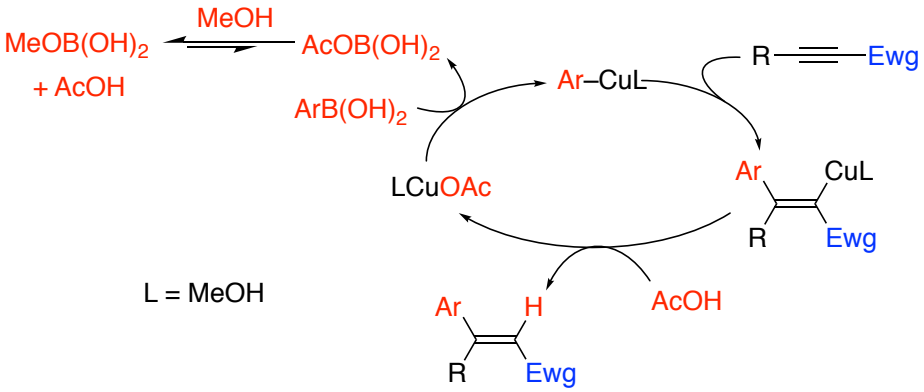

Scheme 12. Modified catalytic cycle for copper-catalyzed hydroarylation.

ASSOCIATED CONTENT

Supporting Information

The Supporting Information is available free of charge on the ACS Publication website.

Figures S1–5, Schemes S1–2, and Tables S1–2 (PDF)

Cartesian coordinates of calculated molecules (PDF)

AUTHOR INFORMATION

Corresponding Author

*E-mail: yamamoto-yoshi@ps.nagoya-u.ac.jp

Notes

The authors declare no competing financial interest.

ACKNOWLEDGMENTS

This research is partially supported by the Platform Project for Supporting Drug Discovery and Life Science Research (AMED) and JSPS KAKENHI (Grand Number JP 16KT0051).

REFERENCES

1. Yamamoto, Y. in *Catalytic Hydroarylation of Carbon–Carbon Multiple Bonds* (Eds.: Ackermann, L.; Gunnoe, T. B.; Habgood, L. G.), Wiley-VCH, Weinheim, **2017**, Chap. 1.7, pp. 305-359.

2. Hayashi, T.; Inoue, K.; Taniguchi, N.; Ogasawara, M. Rhodium-Catalyzed

Hydroarylation of Alkynes with Arylboronic Acids: 1,4-Shift of Rhodium from 2-Aryl-1-alkenylrhodium to 2-Alkenylarylrhodium Intermediate. *J. Am. Chem. Soc.* **2001**, *123*, 9918.

3. Shirakawa, E.; Takahashi, G.; Tsuchimoto, T.; Kawakami, Y. Nickel-catalyzed hydroarylation of alkynes using arylboron compounds: selective synthesis of multisubstituted arylalkenes and aryldienes. *Chem. Commun.* **2001**, 2688.
4. Robbins, D. W.; Hartwig, J. F. A Simple, Multidimensional Approach to High-Throughput Discovery of Catalytic Reactions. *Science* **2011**, *333*, 1423.
5. Lin, P.-S.; Jeganmohan, M.; Cheng, C.-H. Cobalt(II)-Catalyzed Regio- and Stereoselective Hydroarylation of Alkynes with Organoboronic Acids. *Chem. Eur. J.* **2008**, *14*, 11296.
6. (a) Yamamoto, Y.; Kirai, N.; Harada, Y. Cu-catalyzed stereoselective conjugate addition of arylboronic acids to alkynoates. *Chem. Commun.* **2008**, 2010. (b) Yamamoto, Y.; Asatani, T.; Kirai, N. Copper-Catalyzed Stereoselective Hydroarylation of 3-Aryl-2-propynenitriles with Arylboronic Acids. *Adv. Synth. Catal.* **2009**, *351*, 1243.

7. (a) Kirai, N.; Yamamoto, Y.; Wipf, P.; Vowell, C. L. Stereoselective Synthesis of 3-Arylacrylates by Copper-Catalyzed Syn Hydroarylation [(*E*)-Methyl 3-phenyloct-2-enoate]. *Org. Synth.* **2010**, *87*, 53. (b) Yamamoto, Y. Discussion Addendum for: Stereoselective Synthesis of 3-Arylacrylates by Copper-Catalyzed Syn Hydroarylation [(*E*)-Methyl 3-phenyloct-2-enoate]. *Org. Synth.* **2018**, *95*, 267.

8. (a) Yamamoto, Y.; Kirai, N. Synthesis of 4-Arulcoumarins via Cu-Catalyzed Hydroarylation with Arylboronic Acids. *Org. Lett.* **2008**, *10*, 5513. (b) Yamamoto, Y.; Yamada, S.; Nishiyama, H. Synthesis of 3-Arylindole-2-carboxylates *via* Copper-Catalyzed Hydroarylation of *o*-Nitrophenyl-Substituted Alkynoates and Subsequent Cadogan Cyclization. *Adv. Synth. Catal.* **2011**, *353*, 701. (c) Murayama, T.; Shibuya, M.; Yamamoto, Y. Synthesis of 4-Aryl-2-Quinolones *via* Copper-Catalyzed Hydroarylation of (*o*-Aminophenyl)propiolates with Arylboronates. *Adv. Synth. Catal.* **2016**, *358*, 166.

9. Yamamoto, Y.; Ohkubo, E.; Shibuya, M. Selective synthesis of trisubstituted (trifluoromethyl)alkenes *via* ligand-free Cu-catalyzed *syn* hydroarylation, hydroalkenylation and hydroallylation of (trifluoromethyl)alkynes. *Green Chem.*

2016, *18*, 4628.

10. (a) Lipshutz, B. H.; Sengupta, S. ORGANOCOPPER REAGENTS: SUBSTITUTION, CONJUGATE ADDITION, CARBO/METALLOCUPRATION, AND OTHER REACTIONS. *Org. React.* **1992**, *41*, 135. (b) Yoshikai, N.; Nakamura, E. Mechanisms of Ncleophilic Organocopper(I) Reactions. *Chem. Rev.* **2012**, *12*, 2339.

11. Gaussian 16, Revision B.01, Frisch, M. J.; Trucks, G. W.; Schlegel, H. B.; Scuseria, G. E.; Robb, M. A.; Cheeseman, J. R.; Scalmani, G.; Barone, V.; Petersson, G. A.; Nakatsuji, H.; Li, X.; Caricato, M.; Marenich, A. V.; Bloino, J.; Janesko, B. G.; Gomperts, R.; Mennucci, B.; Hratchian, H. P.; Ortiz, J. V.; Izmaylov, A. F.; Sonnenberg, J. L.; Williams-Young, D.; Ding, F.; Lipparini, F.; Egidi, F.; Goings, J.; Peng, B.; Petrone, A.; Henderson, T.; Ranasinghe, D.; Zakrzewski, V. G.; Gao, J.; Rega, N.; Zheng, G.; Liang, W.; Hada, M.; Ehara, M.; Toyota, K.; Fukuda, R.; Hasegawa, J.; Ishida, M.; Nakajima, T.; Honda, Y.; Kitao, O.; Nakai, H.; Vreven, T.; Throssell, K.; Montgomery, J. A., Jr.; Peralta, J. E.; Ogliaro, F.; Bearpark, M. J.; Heyd, J. J.; Brothers, E. N.; Kudin, K. N.; Staroverov, V. N.; Keith, T. A.; Kobayashi, R.;

Normand, J.; Raghavachari, K.; Rendell, A. P.; Burant, J. C.; Iyengar, S. S.; Tomasi, J.; Cossi, M.; Millam, J. M.; Klene, M.; Adamo, C.; Cammi, R.; Ochterski, J. W.; Martin, R. L.; Morokuma, K.; Farkas, O.; Foresman, J. B.; Fox, D. J. Gaussian, Inc., Wallingford CT, 2016.

12. (a) Zhao, Y.; Truhlar, D. G. Density Functionals with Broad Applicability in Chemistry. *Acc. Chem. Res.* **2008**, *41*, 157. (b) Zhao, Y.; Truhlar, D. G. The M06 suite of density functionals for main group thermochemistry, thermochemical kinetics, noncovalent interactions, excited states, and transition elements: two new functionals and systematic testing of four M06-class functionals and 12 other functionals. *Theor. Chem. Acc.* **2008**, *120*, 215.

13. Hay, P. J.; Wadt, W. R. *Ab initio* effective core potentials for molecular calculations. Potentials for K to Au including the outermost core orbitals. *J. Chem. Phys.* **1985**, *82*, 299.

14. (a) Hehre, W. J.; Ditchfield, R.; Pople, J. A. Self-Consistent Molecular Orbital Methods. XII. Further Extensions of Gaussian-Type Basis Sets for Use in Molecular Orbital Studies of Organic Molecules. *J. Chem. Phys.* **1972**, *56*, 2257. (b) Hariharan,

P. C.; Pople, J. A. The influence of polarization functions on molecular orbital hydrogenation energies. *Theor. Chim. Acta* **1973**, *28*, 213. (c) Fracl, M. M.; Pietro, W. J.; Hehre, W. J.; Binkley, J. S.; Gordon, M. S.; DeFrees, D. J.; Pople, J. A. Self-consistent molecular orbital methods. XXIII. A polarization-type basis set for second-row elements. *J. Chem. Phys.* **1982**, *77*, 3654.

15. (a) Fukui, K. The Path of Chemical Reactions – The IRC Approach. *Acc. Chem. Res.* **1981**, *14*, 363. (b) Gonzalez, C.; Schlegel, H. B. An improved algorithm for reaction path following. *J. Chem. Phys.* **1989**, *90*, 2154. (c) Gonzalez, C.; Schlegel, H. B. Reaction path following in mass-weighted internal coordinates. *J. Phys. Chem.* **1990**, *94*, 5523.

16. (a) Kohn, W.; Becke, A. D.; Parr, R. G. Density Functional Theory of Electronic Structure. *J. Phys. Chem.* **1996**, *100*, 12974. (b) Stephen, P. J.; Devlin, F. J.; Chabalowski, C. F.; Frisch, M. Ab Initio Calculation on Vibrational Absorption and Circular Dichroism Spectra Using Density Functional Force Fields. *J. Phys. Chem.* **1994**, *98*, 11623. (c) Becke, A. D. Density-functional thermochemistry. III. The role of exact exchange. *J. Chem. Phys.* **1993**, *98*, 5648. (d) Lee, C.; Yang, W.; Parr, R. G.

Development of the Colle—Salvetti correlation-energy formula into a functional of the electron density. *Phys. Rev. B* **1988**, *37*, 785.

17. Andrae, D.; Häussermann, U.; Dolg, M.; Stoll, H.; Preuß, H. Energy-adjusted *ab initio* pseudopotentials for the second and third row transition elements. *Theor. Chim. Acta* **1990**, *77*, 123.

18. Martin, J. M. L.; Sundermann, A. Correlation consistent valence basis sets for use with the Stuttgart–Dresden–Bonn relativistic effective core potentials: The atoms Ga–Kr and In–Xe. *J. Chem. Phys.* **2001**, *114*, 3408.

19. (a) Krishnan, R.; Binkley, J. S.; Seeger, R.; Pople, J. A. Self-consistent molecular prbital methods. XX. A basis set for correlated wave functions. *J. Chem. Phys.* **1980**, *72*, 650. (b) McLean, A. D.; Chandler, G. S. Contracted Gaussian basis sets for molecular calculations. I. Second row atoms, Z = 11–18. *J. Chem. Phys.* **1980**, *72*, 5639. (c) Frisch, M. J.; Pople, J. A.; Binkley, J. S. Self-consistent molecular orbital methods 25. Supplementary functions for Gaussian basis sets. *J. Chem. Phys.* **1984**, *80*, 3265. (d) Clark, T.; Chandrasekhar, J.; Spitznagel, G. W.; Schleyer, P. v. R.

Efficient diffuse function-augmented basis sets for anion calculations. III. The 3-21+G basis set for first-row elements, Li–F. *J. Comp. Chem.* **1983**, *4*, 294.

20. Grimme, S.; Ehrlich, S.; Goerigk, L. Effect of the damping function in dispersion corrected density functional theory. *J. Comp. Chem.* **2011**, *32*, 1456.

21. Marenich, A. V.; Cramer, C. J.; Truhlar, D. G. Universal Solvation Model Based on Solute Electron Density and on a Continuum Model of the Solvent Defined by the Bulk Dielectric Constant and Atomic Surface Tensions. *J. Phys. Chem. B* **2009**, *113*, 6378.

22. CYLview, 1.0b; Legault, C. Y., Université de Sherbrooke, 2009 (http://www.cylview.org).

23. As a possibility, bimetallic reductive elimination might occur from two $ArCu^{II}OAc$ species to produce 2 equivs of $Cu^{I}OAc$ with one equiv of a biaryl as we previously proposed in our study on copper-catalyzed homocoupling of arylboronic acids (Kirai, N.; Yamamoto, Y. Homocoupling of Arylboronic Acids Catalyzed by 1,10-Phenanthroline-Ligated Copper Complexes in Air. *Eur. J. Org. Chem.* **2009**, 1864). DFT calculations of model phenylcopper(II) species suggest that there are two

dimeric complexes, triplet **S1** and singlet **S2**, in which PhCu(OCHO) fragments are arranged in an antiparallel fashion, and singlet **S2** is much more stable than triplet **S1** (Figure S1, Supporting Information). A triplet complex with a parallel arrangement, **S3**, could be located 12.8 kcal/mol lower in energy than triplet **S1**. In striking contrast, the structural optimization of the corresponding singlet complex resulted in the significantly exergonic formation of biphenyl complex **S4**, in which one of the two coper centers forms a η^2-arene complex. Thus, bimetallic reductive elimination is expected to be facile.

24. Tresse, C.; Guissart, C.; Schweizer, S.; Bouhoute, Y.; Chany, A.-C.; Goddard, M.-L.; Blanchard, N.; Evano, G. Practical Methods for the Synthesis of Trifluoromethylated Alkynes: Oxidative Trifluoromethylation of Copper Acetylides and Alkynes. *Adv. Synth. Catal.* **2014**, *356*, 2051.

25. Unpublished result.

26. Hansch, C.; Leo, A.; Taft, R. W. A survey of Hammett substituent constants and resonance and field parameters. *Chem. Rev.* **1991**, *91*, 165.

27. Westmark, P. R.; Gardiner, S. J.; Smith, B. D. Selective Monosaccharide Transport through Lipid Bilayers Using Boronic Acid Carriers. *J. Am. Chem. Soc.* **1996**, *118*, 11093.

28. Pal, R. Boric acid in organic synthesis: scope and recent developments. *Arkivoc* **2018**, *part I*, 346.

29. (a) Nilsson, K.; Andersson, T.; Ullenius, C.; Gerold, A.; Krause, N. NMR Spectroscopic Investigation of the Adducts Formed by Addition of Cuprates to Ynoates and Ynones: Alkenylcuprates or Allenolates? *Chem. Eur. J.* **1998**, *4*, 2051. (b) Ahlquist, M.; Nielsen, T. E.; Le Quement, S.; Tanner, D.; Norrby, P.-O. An Experimental and Theoretical Study of the Mechanism of Stannylcupration of α,β-Acetylenic Ketones and Esters. *Chem. Eur. J.* **2006**, *12*, 2866.

30. Because a small imaginary frequency (13.7507i cm^{-1}) associated with the rotational vibration mode of the methyl group on the acetate ligand could not be removed, the optimization of **TS$_{23\text{-}24}$** and subsequent IRC calculation were carried out with the constraint on the methyl rotation.

31. Kozuch, S.; Shaik, S. How to Conceptualize Catalytic Cycles? The Energetic Span Model. *Acc. Chem. Res.* **2011**, *44*, 101.

32. Transmetalation involving $Cu(OAc)_2$ and organoboron compounds has been proposed in Chan–Lam–Evans-type coupling reactions (Neuville, L. in *Copper-Mediated Cross-Coupling Reactions* (Eds.: Evano, G.; Blanchard, N.), Wiley-VCH, Weinheim, **2014**, Chap. 4, pp. 113-185). The alcoholysis of acetoxy pinacol borate (AcOBpin) was proposed to generate acetic acid (Shade, R. E.; Hyde, A. M.; Olsen, J.-C.; Merlic, C. A. Copper-Promoted Coupling of Vinyl Boronates and Alcohols: A Mild Synthesis of Allyl Vinyl Ethers. *J. Am. Chem. Soc.* **2010**, *132*, 1202).